CELLULOSE/GRAPHENE NANOPLATELETS CRYOGEL FOR ADSORPTION OF DYES IN AN AQUEOUS MEDIUM

LÍDIA K. LAZZARI,[*,**] ADEMIR J. ZATTERA[**] and RUTH M. C. SANTANA[*]

[*]*Postgraduate Program in Mining, Metallurgical and Materials Engineering, Federal University of Rio Grande do Sul (UFRGS), Porto Alegre, Brazil*
[**]*Postgraduate Program in Process Engineering and Technologies, University of Caxias do Sul (UCS), Caxias do Sul, Brazil*
✉ *Corresponding author: L. K. Lazzari, lidia_lazzari@yahoo.com.br*

Contamination of water resources by industrial dyes has caused environmental, economic and human health hazards. There is a great need to find effective technologies to remove pollutants in a safe and accessible way. An enticing option involves employing cellulose cryogels as adsorbents to extract dyes from water. This research delves into the production intricacies of cellulose/graphene cryogels and meticulously explores their physical and chemical properties. Dye adsorption tests were conducted to evaluate the efficiency of the prepared cryogels in removing organic dyes from water. The results show that cryogels have high dye adsorption capacity, especially when combined with graphene nanoplatelets. Kinetic and isothermal models reveal that the adsorption process follows pseudo-second-order kinetics and is described by the Langmuir isotherm, suggesting a single-layer adsorption mechanism and a strong interaction between the dyes and the cryogels. In summary, the study demonstrates that the cellulose/graphene nanoplatelets cryogels are effective in removing organic dyes from water, offering a sustainable and economically viable solution to the problem of industrial dye pollution.

Keywords: cryogel, cellulose, graphene nanoplatelets, adsorption, dyes

INTRODUCTION

Water is an essential natural resource for human life and for the entire planet, as well as an important strategic resource for the sustainable development of the economy. With the development of science and technology and the continuous advance of industrialization, water pollution problems have become more and more prominent. The worsening of water resources pollution resulting from industrial and domestic discharges, leaks or spills of inappropriate chemical products constitute the main challenges faced by society, because of the sanitary, environmental and economic aspects involved.[1,2]

Polluted water has harmful effects on the marine ecosystem, causing waterborne diseases, negatively affecting biodiversity and leading to infertility of agricultural land. In recent decades, water polluted by dye contamination has caused serious environmental safety risks and threats to the long-term sustainable evolution of human society. It is a global concern that large amounts of dyes are discharged into groundwater every year from the textile, leather, paper, plastics industries *etc*.[1,2,3] Most synthetic dyes are composed of a complex structure based on the polycyclic aromatic group, they are very stable and are not easily degraded naturally, as they are resistant to aerobic digestion and microbial degradation.[1]

It is estimated that the biggest generator of colored wastewater is the textile industry. Approximately 20% of the dye used to dye textile fibers is not fixed and is discharged as effluent, resulting in a high level of pollution. However, environmental damage does not depend exclusively on the amount of dye discharged, but also on the mixture of dyes with other substances, all of which have toxic properties that make up the industrial effluent.[4] The contamination of water resources by dyes confers toxicity to aquatic life and human assimilation through the food chain, which can cause serious diseases to

humans, affecting the kidneys, central nervous system, liver, *etc.*[1,5,6]

It is really an urgent matter to find an effective technology to remove dye contamination safely and easily from water. Reducing the cost of the treatment and removing the highest percentage of pollutants before the effluent is released into water bodies has been the focus of several studies, including chemical, physical, biochemical, biological and hybrid processes. In this sense, treatments that combine physical, chemical and biological processes are common to reduce pollutants in industrial effluents. Physical processes are the most frequently encountered when it comes to dye removal, being a viable option for dyes that generate more toxic products during the treatment than the original dyes.[4]

Adsorption is the surface phenomenon where the adsorbate molecules are attracted to the surface of the adsorbent, without changing their chemical composition.[7] Adsorption is recognized as one of the most efficient approaches for the removal of dyes from water, having particular advantages, such as low cost, high efficiency, easy operation, eco-friendliness and no formation of harmful substances during the treatment. The objectives in developing adsorbents for removing dyes from water include achieving high efficiency and low cost.[2,8,9]

The use of natural raw materials, such as cellulose or agro-industrial residues, for the manufacture of adsorbents for the removal of pollutants from water, has many attractive characteristics, contributing to the reduction of costs for the elimination of residues, thus contributing to environmental protection.[10] As a natural and organic polymer, cellulose is present in the cell walls of plants, particularly in stems, stalks and trunks and in all woody portions of plant tissues. Also, it is present in bacteria, fungi, algae and even in animals. Coming from a natural cycle, cellulose is considered a renewable natural resource and an almost inexhaustible source of raw material for the growing demand for environmentally friendly and biodegradable products.[11,12]

Cellulose cryogels have been considered as a promising and sustainable material for adsorption and separation of organic dyes from polluted water. Although they have been in the focus in the field of adsorption of organic dyes due to their unique structure and inherent characteristics, their adsorption capacity towards toxic compounds is often limited. On the other hand, carbon-based porous materials are considered ideal adsorbents for water treatment, due to their chemical inertness properties, good mechanical stability, homogeneous components and low content of contaminants.[1,5,13] Considering this, several authors have reported research on the development of cellulose aerogels and allotropic forms of carbon, such as graphene oxide[8,14,15] and carbon nanotubes[16,17] for different applications. However, the large amount of chemical products required and the generation of acid residues during the synthesis of these precursors, associated with complex and expensive technologies, in addition to the equipment involved in the preparation, restrict their large-scale production.[14,16,18] The addition of these carbon-based materials to the formulation of the aerogels has been reported to impart properties such as hydrophobicity and compressibility to the aerogels.[8,19]

The use of graphene nanoplates in cellulose cryogels offers a series of advantages. Firstly, graphene is known for its high electrical and thermal conductivity, as well as its exceptional mechanical strength. By incorporating graphene nanoplatelets into cellulose aerogels, it is possible to significantly improve their mechanical and load transport properties, making them more effective as adsorbents for the removal of contaminants, such as dyes, in the indicated case. Furthermore, graphene can contribute to increasing the surface area and porosity of cellulose cryogels, thus expanding their capacity to adsorb and remove pollutants from water. In summary, the addition of graphene nanoplatelets enhances the properties of cellulose cryogels, making them a promising alternative for various environmental and water purification applications.[2,5,6,9]

With these considerations, the objective of the present proposal is to use graphene nanoplatelets (GNPs) as reinforcement in cellulose cryogels. The novelty of this work is to bring a simple and low-cost methodology, unlike those reported in the articles mentioned above, for the production of cellulose/graphene cryogels, without the use of chemical reagents, with the objective of developing an adsorbent material with potential to be used for the removal of dyes from aqueous media.

EXPERIMENTAL
Materials

Unbleached long fiber type (FLNB) cellulose obtained from *Pinus elliottii* species, utilized in this study, was provided by Trombini Company, located in Fraiburgo, SC. The graphene nanoplatelets (grade 06–0220) were purchased from Strem Chemicals (MA, USA), with 6–8 nm in thickness and 25 μm in diameter, with >99.5% C according to the manufacturer.

Cellulose/GNP cryogel production

The cellulose/GNP cryogels were fabricated following the methodology outlined in our prior research.[20] In summary, cellulose was mixed with distilled water at a concentration of 1.5% w/w. Subsequently, this mixture underwent grinding in a stone mill (Masuko Sangyo – model MKCA6-2J, Japan) to break down the fibers. The grinding process was facilitated by an open rotor centrifugal pump, which circulated the suspension for 5 hours at a rotation speed of 2500 rpm.

Upon acquiring the cellulose suspension, it was subjected to centrifugation for 5 minutes at 4500 rpm. Graphene nanoplatelets (GNP) were introduced to the supernatant at concentrations of 2.5% w/w relative to the cellulose concentration, and the mixture was subjected to mechanical agitation for 5 minutes to ensure homogeneity. Next, the supernatant was combined with the sediment and mechanically shaken for an additional 5 minutes. The resulting suspension underwent sonication for 5 minutes, followed by freezing in an ultra-freezer at -80 °C for 24 hours. Subsequently, it underwent lyophilization in a lyophilizer (Liobrás – model LioTop L101, Brazil) for approximately 72 hours. The cryogels were designated as cell_C for cellulose cryogel and cell_GNP for cellulose cryogel with GNP.

Cellulose/GNP cryogel caracterization

Apparent density was assessed following ASTM D1622-08 (Eq. 1), while porosity was determined using Equation (2):

$$\rho_{cryogel} = \frac{m_c}{v_c}$$
(1)

where $\rho_{cryogel}$ = specific mass of the cryogel (g cm^{-3}); m_c = cryogel mass (g) and v_c = cryogel volume (cm^3).

$$Porosity\ (\%) = \left(1 - \frac{\rho_{cryogel}}{\rho_{cellulose}}\right) x100$$
(2)

where $\rho_{cryogel}$ = specific mass of the cryogel (g cm^{-3}) and $\rho_{cellulose}$ = specific mass of cellulose (0.532 g.cm^{-3}).

The cryogel morphology was examined via SEM-FEG using a Tescan microscope, model FEG Mira 3, sourced from Czech Republic. This analysis also makes it possible to visualize the fiber diameters. Because the cryogel was produced from a non-conductive material, it was necessary to carry out a deposition of gold on the samples for about 1 min. The accelerating voltage to be used in this analysis is 15 kV.

The organic dye adsorption tests were carried out in a synthetic solution with Congo Red dye with an initial concentration of 5 mg L^{-1}. The tests were carried out for a total duration of 24 h, at 25 °C under agitation. A calibration curve was performed to determine the relationship between absorbance and concentration. After an appropriate time, the residual amounts of dyes (mg L^{-1}) in the solution were determined using a UV-visible spectrophotometer at a wavelength of 498 nm. The removal efficiency or dye adsorption efficiency (A%) was calculated according to Equation (3):

$$A\% = \frac{C_o - C_f}{C_o} x100$$
(3)

where C_0 and C_f is the initial and final concentrations (mg L^{-1}) of dye present in the solution, respectively.[3,24]

The Congo Red dye adsorption kinetics were investigated to evaluate the adsorption capacity of the dye by the cryogel as a function of the contact time. Initially, the maximum capacity of dye adsorption by the cryogel was determined, so as to carry out the study of the adsorption kinetics afterwards. To this end, dye concentrations were determined in order to represent the capacity of dye removal from the medium between 10 and 120%. To determine the constants of adsorption rate and adsorption capacity at equilibrium, the pseudo-first (Eq.4) and pseudo-second order (Eq.5) kinetic equations were used:

$$q_t = q_e(1 - e^{k_1 t})$$
(4)

$$q_t = \frac{k_2 q_e^2 t}{1 + k_2 q_e t}$$
(5)

where q_t is the amount of solute adsorbed (mg g^{-1}) in time t, q_e is the amount of solute adsorbed (mg g^{-1}) at equilibrium, k_1 (min^{-1}) is the constant of the pseudo-first order equation and k_2 (mg g^{-1} min^{-1}) is the constant of the pseudo-second order equation.

Adsorption isotherms describe the phenomenon that governs the retention of a substance in an aqueous medium on a solid phase at a constant temperature. They show the equilibrium relationship between fluid concentration and adsorbent particle concentration at a given temperature. Thus, it is possible to estimate the maximum amount of solute that the solid will adsorb, the economic viability of the adsorbent for the purification of the liquid and the behavior of the adsorbent during the adsorption process.[7,21] The Langmuir and Freundlich isotherms were studied according to the nonlinear regressions presented in Equations (6) and (7), respectively:

$$q_e = \frac{K_L Q_m C_e}{1 + K_L C_e}$$
(6)

$$q_e = K_F C_e^{1/n}$$

(7)

where C_e is the equilibrium concentration (mg L^{-1}), q_e is the amount of solute adsorbed (mg g^{-1}) at equilibrium, Q_m – theoretical maximum adsorption capacity that corresponds to a monolayer coating (mg g^{-1}), K_L is the Langmuir isotherm constant (L g^{-1}), and K_F (g g^{-1} (g L^{-1})-1/n) and n are constants that depend on the temperature and are related to the adsorption capacity and intensity, respectively.

RESULTS AND DISCUSSION
Cryogels characterization

Table 1 shows the characterization results of two types of cryogels, cell_C and cell_GNP. The apparent density of cell_GNP (0.020 ± 0.002 g cm^{-3}) was slightly higher than that of cell_C (0.017 ± 0.003 g cm^{-3}), indicating that the addition of graphene nanoplatelets (GNPs) increased the overall density of the cryogel. The porosity of both cryogels was quite high, with cell_C having a porosity of 96.7 ± 0.5% and cell_GNP having a porosity of 96.2 ± 0.4%. The apparent density found is similar to that reported for other cellulose cryogels.[20,22]

The high porosity of the cryogels is desirable for many applications as it provides a large surface area for interactions with surrounding molecules or cells. However, the slightly lower porosity of cell_GNP may suggest that the addition of GNPs affects the overall structure of the cryogel. This could have implications for the functional performance of the cryogel in applications such as drug delivery or tissue engineering.

The cryogels present a 3D structure, with agglomerated cellulose fibers, due to the hygroscopic characteristic of cellulose (Fig. 1). In Figure 1 (d), it is possible to identify the GNP adhered to the surface of the cellulose fibers. Cellulose/GNP cryogels are generally highly porous materials, with a three-dimensional structure of interconnected pores.

Table 1
Characterization of cryogels

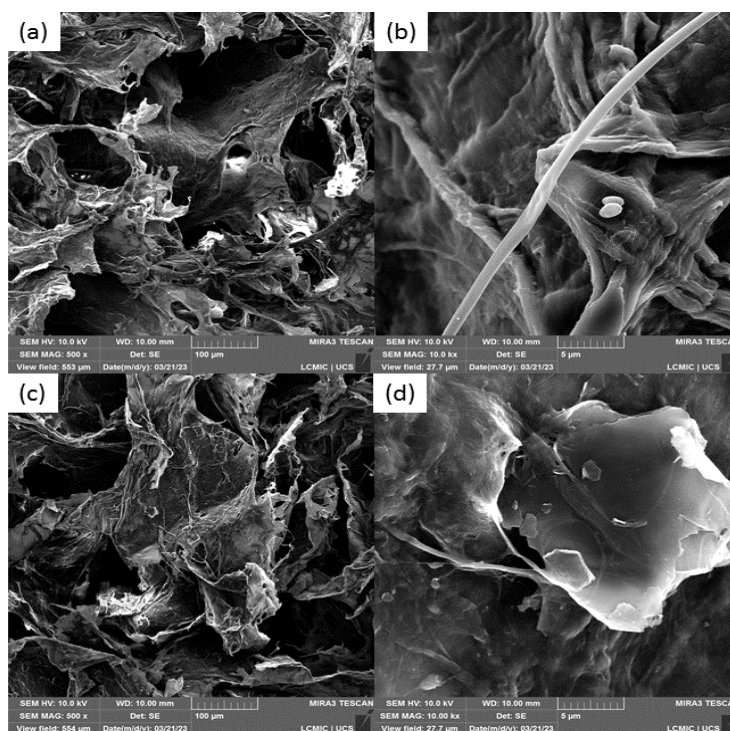| Cryogel	cell_C	cell_GNP
Apparent density (g cm^{-3})	0.017 ± 0.003	0.020 ± 0.002
Porosity (%)	96.7 ± 0.5	96.2 ± 0.4

Figure 1: Micrographs of cryogels: (a) cell_C at 500x, (b) cell_GNP at 500x, (c) cell_C at 10 kX and (d) cell_GNP at 10 kX

Cellulose is a natural polysaccharide that forms fibers that aggregate and form a porous network. Graphene is a form of carbon consisting of a flat layer of carbon atoms arranged in a hexagonal lattice. When combined, they form a cryogel that exhibits porosity at different scales. Cellulose contributes larger pore sizes, while GNP contributes smaller pores. The porous structure of cryogels is determined by the manufacturing technique, which involves forming a cellulose network and adding graphene nanoparticles. During the drying process, the solvent is removed and the nanoparticles aggregate to form a high specific surface porous network.[23-25]

Adsorption properties of cryogels

The cellulose/GNP cryogels are super-resilient in aqueous media, as previously reported, and do not change shape during dye adsorption. The adsorption of the Congo Red dye is shown in Figure 2, where the initial dye concentrations were varied to determine the adsorption capacity of the cryogel. The maximum initial concentration used was 50 mg/L (concentrations greater than 50 mg/L exceed the absorbance reading capacity of the equipment).

According to the results found, for the initial dye concentration of 5.0 mg/L, the cell_GNP cryogel showed a higher adsorption capacity than the cell_C cryogel of 4.49 and 4.23 mg L, respectively. These results show a dye removal

from the solution of 89% for the cell_GNP cryogel and 83% for the cell_C cryogel.

With the increase in the initial concentration of the dye, the adsorption capacity of the cell_GNP cryogel also increases, reaching a maximum capacity of 26.8 mg L^{-1}, but with the increase in the initial concentration of the dye, the percentage of its removal decreases, being only 54% for Co = 50 mg L^{-1}. As seen in Figure 2 (a), the system reaches equilibrium around 300 min of the test, *i.e.*, after this period, dye adsorption is small to justify the permanence of contact between adsorbent and solution for a period of more than 5 hours.

The non-linear regression of the pseudo-first and pseudo-second order kinetic equations were applied to the Congo Red dye adsorption curves, as shown in Figure 3.

Table 2 presents the data of the kinetic parameters of the pseudo-first and pseudo-second order adsorption models for the removal of Congo Red dye using cellulose and graphene cryogels. The initial dye concentration (Co) ranged from 2.5 to 50 g L^{-1}.

The q_e (maximum adsorption capacity) values obtained from the pseudo-first order model increased with increasing initial dye concentration for both cryogels. The values of k_1 (adsorption rate constant) decreased with increasing initial dye concentration, indicating that the adsorption rate decreases as the dye concentration increases.
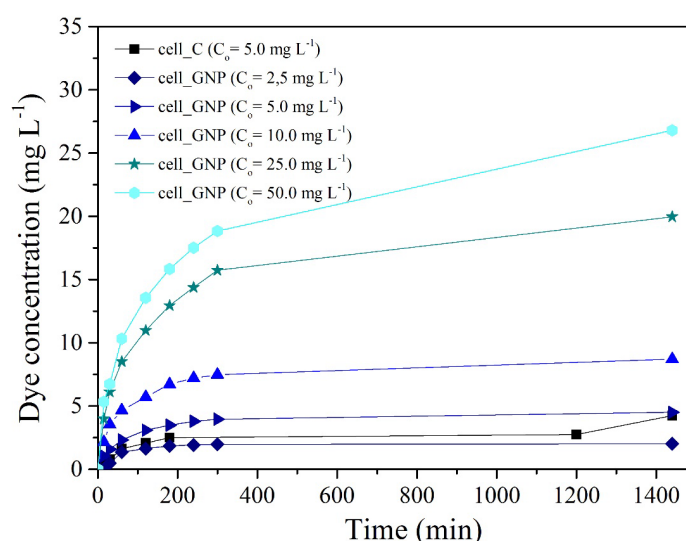

Figure 2: (a) Kinetics of dye adsorption onto cellulose/GNP cryogels for different initial dye concentrations
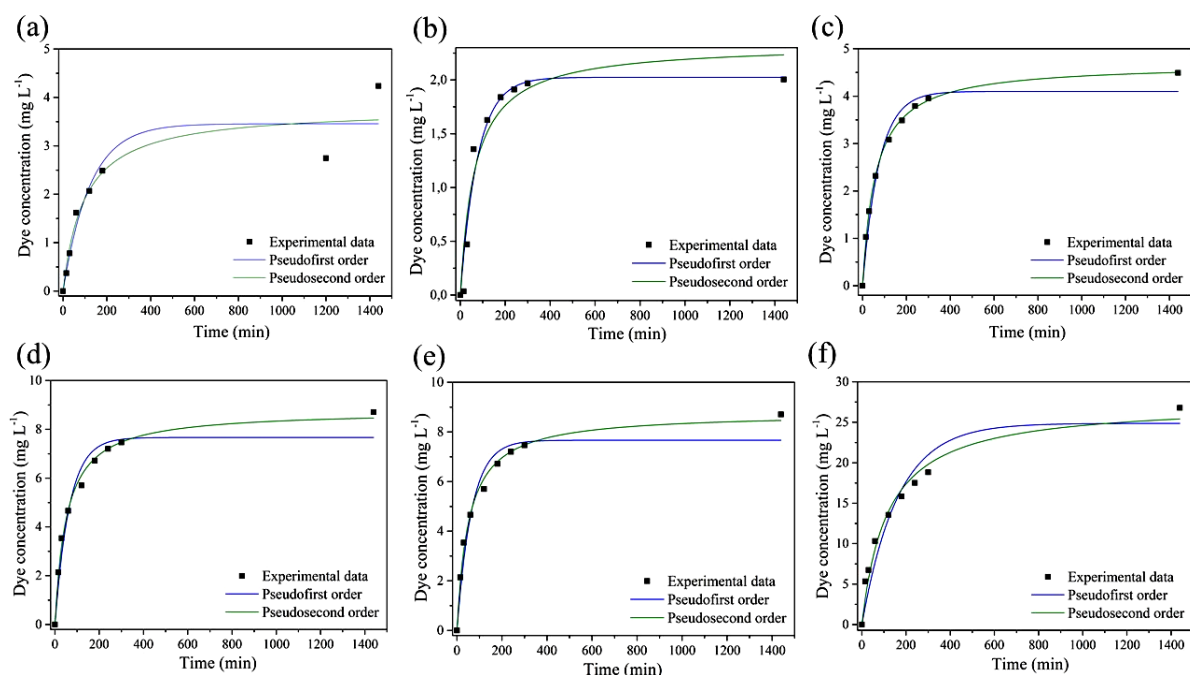
Figure 3: Nonlinear regression for the reactive kinetic models of pseudo-first and pseudo-second order:
(a) cell_C (5.0 mg L^{-1}); (b) cell_GNP (2.5 mg L^{-1}); (c) cell_GNP (5.0 mg L^{-1}); (d) cell_GNP (10.0 mg L^{-1});
(e) cell_GNP (25.0 mg L^{-1}); and (f) cell_GNP (50.0 mg L^{-1})

In the pseudo-second order model, q_e values also increased with increasing initial dye concentration for both cryogels, but k_2 (adsorption rate constant) values significantly decreased with increasing initial dye concentration. Furthermore, the second-order model showed a better fit to the data than the first-order model, as indicated by the R^2 adj values.

The kinetic parameters are shown in Table 2, and the ability of equilibrium adsorption at Co = 50 mg L^{-1} was q_e = 27 mg g^{-1} for the cell_GNP cryogel. The equation that most correlates to the system is the pseudo-second order kinetic equation, as it presented the R^2_{adj} closest to 1

(>0.97). This indicates a good regression fit and that this model better predicts the adsorption behavior in this situation; adsorption being more efficient at lower dye concentrations. This information is important to optimize the process of removing toxic dyes from industrial effluents. Furthermore, it means that both external and intraparticle diffusion steps control the total kinetics of the adsorption process.[26]

The results regarding the equilibrium of the adsorption process for the studied temperature (23 °C) and the adjustments to the Langmuir and Freundlich isotherm models, based on non-linear regression analysis are shown in Figure 4.

Table 2
Kinetic parameters of pseudo-first and pseudo-second order reaction models of adsorption of Congo Red dye on cryogels

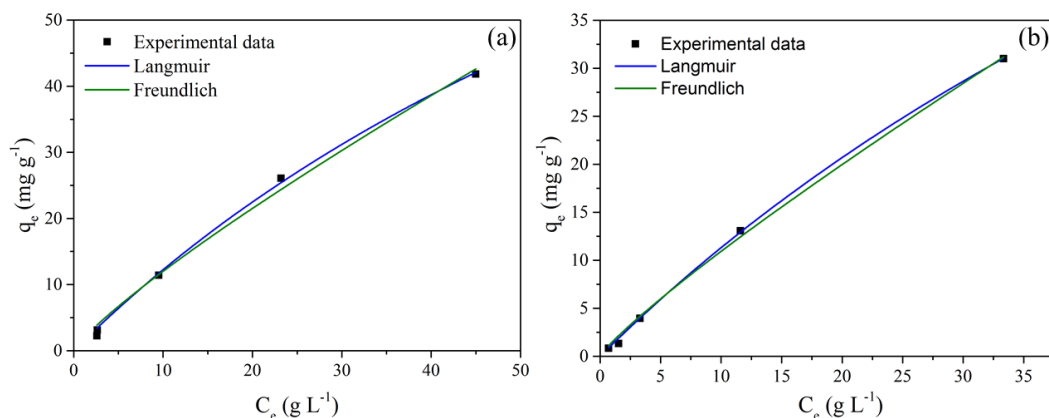|	cell_GNP					cell_C
Co (g.L^{-1})	2.5	5.0	10.0	25.0	50.0	5.0
Pseudo-first order						
q_e	2.02±0.11	4.10±0.15	7.67±0.37	18.21±1.31	24.87±2.07	3.46±0.31
k_1	0.013±0.002	0.013±0.002	0.015±0.003	0.008±0.002	0.006±0.001	0.008±0.002
R^2_{adj}	0.9582	0.9745	0.9499	0.9377	0.9235	0.8955
Pseudo-second order						
q_e	2.33±0.21	4.69±0,04	8.77±0.19	20.39±0.78	27.46±1.48	3.77±0.37
k_2	0.007±0.003	0.003±1.45E-4	0.002±2.31E-4	5.5E-4±8.6E-5	3.13E-4±6.5E-5	0.003±0.001
R^2_{adj}	0.9241	0.9990	0.9931	0.9855	0.9747	0.9057

Figure 4: Nonlinear regression isothermal models of Langmuir and Freundlich: (a) cell_C and (b) cell_GNP

Table 3 presents the results of the fit parameters of the Langmuir and Freundlich adsorption isotherm models for cell_C and cell_GNP cryogels. The Langmuir model is based on the assumption that the adsorbent surface is uniform and that the maximum number of adsorbate molecules that can be adsorbed is finite. The Freundlich model is suitable for heterogeneous surfaces and takes into account the interaction between adsorbed molecules.[7,21]

Analyzing the results presented in Table 3, for the Langmuir model, it was observed that the maximum adsorption capacity (Q_m) was higher for the cell_C cryogel than for the cell_GNP one. As for the Freundlich model, the values of the K_F parameter were higher for the cell_C cryogel than for the cell_GNP one, indicating a greater affinity of cellulose for the Congo red dye.

Although the results show that both models presented a good fit to the experimental data, with high R^2_{adj} values close to unity (i.e. greater than 0.99 for both samples), it is observed that the Langmuir model obtained more satisfactory values of R^2_{adj} compared to the Freundlich model, suggesting a more accurate regression adjustment. Thus, it can be concluded that the Langmuir model is the most adequate to describe the experimental data of dye adsorption by the cellulose and cellulose/GNP cryogels. These results indicate that the adsorption process occurs through the formation of a monolayer, where the cryogel adsorption sites are identical and energetically equivalent, allowing only one molecule to be accommodated at each site.

Table 3
Parameter values of the cryogels adsorption isotherm models

	cell_C	cell_GNP
Langmuir		
R^2_{adj}	0.9976	0.9993
Q_m (g.g^{-1})	139.24±23.99	123.35±15.77
K_L (L.g^{-1})	0.0096±0.0022	0.0101±0.0017
R_L	0.02376–0.2247	0.02375–0.2246
Freundlich		
R^2_{adj}	0.9921	0,9976
K_F (g.g^{-1} (g.L^{-1})$^{-1/n}$)	1.721±0.366	1.469±0.183
n	1.186±0.085	1.148±0.050

After identifying that the Langmuir model is the most adequate to describe the adsorption process, it is important to analyze the constants related to it. The k_L parameter is directly linked to the interaction between the adsorbate and the

adsorbent, and higher k_L values indicate a stronger interaction between the two components.

In their investigation, Mhlongo et al.[27] examined the potential of a cost-effective cationized cellulose material derived from hemp stem and branch fibers for adsorbing Methyl

Orange and Sunset Yellow dyes from aqueous solutions. To functionalize the cellulose, glycidyl trimethylammonium chloride (GTMAC) served as cationizing agent. Their findings indicated that the Langmuir isotherm model offered the most suitable fit for the adsorption of MO onto GT-cellulose, with a correlation coefficient (R^2) of 0.918. This suggests a monolayer adsorption mechanism, indicating a uniform interaction between the dye molecules and the surface of GT-cellulose.

In their investigation, Omer *et al.*[28] examined the potential of biodegradable cellulose derived from sugarcane bagasse for dye removal. The cellulose material was produced through an alkaline treatment, followed by a bleaching method. The researchers found that the adsorption of Crystal Violet and Methylene Blue dyes onto the treated sugarcane bagasse-based cellulose could be accurately described by the Langmuir isotherm model. The maximum adsorption capacities were assessed to be 107.5 mg/g for Crystal Violet and 112.9 mg/g for Methylene Blue. Additionally, the pseudo-second order kinetic model exhibited the most favorable fit for the experimental data, suggesting that chemical mechanisms likely play a substantial role in the adsorption of the dyes onto treated sugarcane bagasse cellulose. This suggests that the adsorption process involves a chemical reaction between the dyes and the cellulose material.

CONCLUSION

The results obtained in this article reveal important characteristics of cellulose and cellulose/GNP cryogels, as well as their effectiveness in the adsorption of Congo Red dye. The characterization of the cryogels revealed a highly connected porous structure, with the addition of graphene nanoparticles, slightly affecting the apparent density and the appearance of the cryogels, but not significantly compromising their porosity. This suggests that the porous structure of the cryogels is maintained, which is crucial for their adsorption properties.

Adsorption results demonstrated that the cellulose/GNP cryogels are highly efficient in dye removal, with a significantly higher adsorption capacity, compared to that of pure cellulose cryogels. Furthermore, the kinetic and isothermal models applied to the adsorption data showed that the pseudo-second order model and the Langmuir model are the most suitable to describe the

adsorption process, indicating a strong and specific interaction between the dyes and the cryogels.

The comparison with other studies also highlights the effectiveness of cellulose cryogels in adsorbing dyes, corroborating the results found in this work. These findings have significant implications for the remediation of water contaminated by industrial dyes, suggesting that cellulose and cellulose/GNP cryogels may be a promising and sustainable solution to the challenges of environmental pollution control.

In summary, the results of this study highlight the potential of cellulose and cellulose/GNP cryogels in removing dyes from water, offering a viable and effective approach for the decontamination of industrial effluents. These findings could be of help in the development of more sustainable and efficient water treatment technologies in the future.

REFERENCES
[1] P. Joshi, O. P. Sharma, S. K. Ganguly, M. Srivastava and O. P. Khatri, *J. Colloid Interface Sci.*, **608**, 2870 (2022), https://doi.org/10.1016/j.jcis.2021.11.016
[2] J. Li, Q. Wang, L. Zheng and H. Liu, *J. Mater. Sci. Technol.*, **41**, 68 (2020), https://doi.org/10.1016/j.jmst.2019.09.019
[3] H. Zhou, R. Chen, J. Wang, J. Lu, T. Yu *et al.*, *Mater. Des.*, **31**, 108947 (2020), https://doi.org/10.1016/j.ijbiomac.2022.01.052
[4] L. D. Ardila-Leal, R. A. Poutou-Piñales, A. M. Pedroza-Rodríguez and B. E. Quevedo-Hidalgo, *Molecules*, **26**, 3813 (2021), https://doi.org/10.3390/molecules26133813
[5] Z. Wang, L. Song, Y. Wang, X. F. Zhang and J. Yao, *J. Phys. Chem. Solids*, **150**, 109839 (2021), https://doi.org/10.1016/j.jpcs.2020.109839
[6] F. Ren, Z. Li, W. Z. Tan, X. H. Liu, Z. F. Sun *et al.*, *J. Colloid Interface Sci.*, **532**, 58 (2018), https://doi.org/10.1016/j.jcis.2018.07.101
[7] K. Y. Foo and B. H. Hameed, *Chem. Eng. J.*, **156**, 2 (2010), https://doi.org/10.1016/j.cej.2009.09.013
[8] C. Xiang, C. Wang, R. Guo, J. Lan, S. Lin *et al.*, *J. Mater. Sci.*, **54**, 1872 (2019), https://doi.org/10.1007/s10853-018-2900-5
[9] F. Jiang, D. M. Dinh and Y. Hsieh, *Carbohyd.*

Polym., **173**, 286 (2017), https://doi.org/10.1016/j.carbpol.2017.05.097

10 A. Bhatnagar and M. Sillanpää, *Chem. Eng. J.*, **157**, 277 (2010), https://doi.org/10.1016/j.cej.2010.01.007

11 D. Klemm, B. Heublein, H. Fink and A. Bohn, *Angew. Chem. Int. Ed.*, **44**, 3358 (2005), https://doi.org/10.1002/anie.200460587

12 A. C. O'Sullivan, *Cellulose*, **4**, 173 (1997), https://doi.org/10.1023/A:1018431705579

13 X. Chang, D. Chen and X. Jiao, *Polymer* (*Guildf*), **51**, 3801 (2010), https://doi.org/10.1016/j.polymer.2010.06.018

14 H. Y. Mi, X. Jing, A. L. Politowicz, E. Chen, H. X. Huang *et al.*, *Carbon N. Y.*, **132**, 199 (2018), https://doi.org/10.1016/j.carbon.2018.02.033

15 C. Wan and J. Li, *Carbohyd. Polym.*, **150**, 172 (2016), https://doi.org/10.1016/j.carbpol.2016.05.051

16 L. Cong, X. Li, L. Ma, Z. Peng, C. Yang *et al.*, *Mater. Lett.*, **214**, 190 (2018), https://doi.org/10.1016/j.matlet.2017.12.015

17 H. C. Hwang, J. S. Woo and S. Y. Park, *Carbohyd. Polym.*, **196**, 168 (2018), https://doi.org/10.1016/j.carbpol.2018.05.013

18 H. Bi, Z. Yin, X. Cao, X. Xie, C. Tan *et al.*, *Adv. Mater.*, **25**, 5916 (2013), https://doi.org/10.1002/adma.201302435

19 J. Li, H. Meng, S. Xie, B. Zhang, J. Li *et al.*, *J. Mater. Chem. A*, **2**, 2934 (2014), https://doi.org/10.1039/c3ta14725h

20 L. K. Lazzari, D. Perondi, A. J. Zattera and R. M. C. Santana, *J. Porous Mater.*, **28**, 279 (2021), https://doi.org/10.1007/s10934-020-00972-3

21 D. J. Shaw, "Introdução à química dos colóides e de superfícies", Sao Paulo, Edgard Blucher LTDA, 1975

22 P. V. O. Toledo, B. F. Martins, C. L. Pirich, M. R. Sierakowski, E. T. Neto *et al.*, *Macromol. Symp.*, **383**, 201800013 (2019), https://doi.org/10.1002/masy.201800013

23 A. K. Kasar, S. Tian, G. Xiong and P. L. Menezes, *J. Porous Mater.*, **29**, 1011 (2022), https://doi.org/10.1007/s10934-022-01230-4

24 M. Zanini, A. Lavoratti, L. K. Lazzari, D. Galiotto, M. Pagnocelli *et al.*, *Cellulose*, **24**, 769 (2017), https://doi.org/10.1007/s10570-016-1142-4

25 C. Hoon, K. Hye, J. Youn and H. Lae, *Cellulose*, **22**, 3715 (2015), https://doi.org/10.1007/s10570-015-0745-5

26 W. Plazinski, W. Rudzinski and A. Plazinska, *Adv. Colloid Interface Sci.*, **152**, 2 (2019), https://doi.org/10.1016/j.cis.2009.07.009

27 J. T. Mhlongo, M. L. Dlamini, Y. Nuapia and A. Etale, *Mater. Today Proc.*, **62**, S133 (2022), https://doi.org/10.1016/j.matpr.2022.02.100

28 A. S. Omer, A. E. G. Naeem, A. I. Abd-Elhamid, O. O. M. Farahat, A. A. El-Bardan *et al.*, *J. Mater. Res. Technol.*, **19**, 3241 (2022), https://doi.org/10.1016/j.jmrt.2022.06.045